JOURNAL OF MATERIALS SCIENCE 19 (1984) 2934–2942

Microstructure evolution and ordering in commercial Mg–PSZ

R. CHAIM, D. G. BRANDON
Department of Materials Engineering, Technion-Israel Institute of Technology, Haifa 32000, Israel

Sintered commercial ZrO_2–9 mol % MgO (PSZ) alloy was heat-treated at different temperatures in the range 900 to 1400° C. The microstructure was studied using transmission electron microscopy (TEM). The as-sintered material was characterized by either fine tetragonal precipitation in cubic matrix grains, or coarser precipitates which had transformed martensitically to the monoclinic symmetry. The diffuse scattering intensity (DSI) was observed to originate from the cubic lattice, and was correlated with the short-range ordering of the oxygen vacancies present in the cubic matrix. However, by annealing at temperatures below 1100° C for relatively short times, long-range ordering occurred in the cubic matrix. The ordered phase was β-$Mg_2Zr_5O_{12}$ with a rhombohedral symmetry, which belongs to the homologous series of $M_nO_{2n-2}(M_7O_{12})$ defect structures derived from the CaF_2-type structure. The ordering process is characteristic only for the cubic regions between the fine-tetragonal precipitates. This microstructure is considered to be a pseudo-equilibrium state and is related to the limited extent of diffusion.

1. Introduction

The polymorphic nature of zirconia (ZrO_2) and the transformations during cooling from cubic (c) to tetragonal (t) and finally to monoclinic (m) structures are now well understood. For technological applications ZrO_2 is usually "alloyed" with cubic oxides, such as MgO, CaO, Y_2O_3 in order to stabilize the high temperature polymorphs (c and t) at ambient temperature.

The presence of the t phase is the principal reason for the improvement in fracture toughness. This phase, which is commonly retained as a metastable phase, can transform to the m symmetry, by a stress-induced martensitic transformation ahead of a crack tip. The ~ 3% volume increase which is involved in this transformation retards crack propagation and results in the toughening effect. Recently, MgO–partially stabilized zirconia (Mg–PSZ) has become important for practical applications. The improved mechanical and electrical properties of Mg-PSZ has led to comprehensive studies of the microstructural development with heat treatment [1–6].

This work describes the micostructural evolution with respect to the pseudo-equilibrium conditions which arise in the commercial Mg–PSZ, followed by the ordering process associated with post-sintering heat treatments.

2. Experimental details

The as-received commercial 9 mol % MgO–ZrO_2 (PSZ) was investigated. Discs 3.0 mm diameter by 0.5 mm thick for different heat treatments were cut using a diamond saw. The heat treatments were carried out in air for the following temperatures and times: 900° C/20 h; 1000° C/5 h; 1100° C/1 h; 1400° C/120 h.

The relatively small size of the samples permitted very fast air cooling outside the furnace, to ensure the retention of the phases and microstructures at the quenching temperature. Several samples were checked by optical ceramography using boiling ammonium-fluoride in water etchant.

A few samples were checked by X-ray diffractometry using Cu$K\alpha$ radiation. TEM samples were thinned mechanically to 80 μm thickness using diamond paste. The final thinning process was the conventional ion-milling process using argon-ion

0022–2461/84 $03.00 + .12

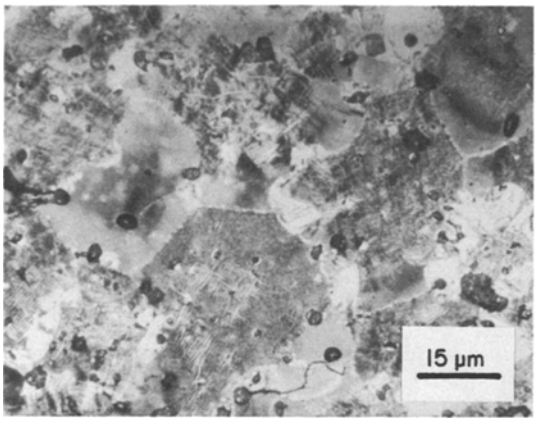

Figure 1 Optical bright-field micrograph (polarized light) of the as-received Mg–PSZ specimen.

bombardment, followed by carbon coating of the TEM specimens.

The transmission electron microscope (TEM)* was operated at 100 kV, using bright-field, dark-field and selected-area diffraction (SAD) modes for the microstructural observations and phase analysis.

3. Results

The composition of the PSZ by chemical wet analysis was determined to be 9 mol % MgO.

An optical micrograph of the as-received (sintered) specimen is shown in Fig. 1. Ignoring porosity (dark dots), the material was composed of matrix grains (grey) and grain-boundary phase (white). More detailed observations in TEM proved these grains to be basically of c symmetry. The c matrix often contain lenticular or ellipsoidal shaped t precipitates with a variable size distribution in different grains (Fig. 2).

However, the homogeneous distribution of these t precipitates hints at a diffusion-controlled nucleation and growth process, crystallographically oriented in the c matrix [1, 6].

The white grain-boundary phase has proved to be large monoclinic twins, as shown in Fig. 3. The presence of a glassy grain-boundary phase was also observed. Appropriate selected-area diffraction patterns (SADP) were used to identify the different phases above. The c grains containing t precipitates exhibited diffuse scattering intensity (DSI), which was proved to be associated with the c matrix using dark-field images. An example of this DSI is illustrated in Fig. 4. No meaningful changes in the optical microstructure were observed for specimens heat treated at 900 to 1100° C. On the other hand, the microstructure of the specimen heat treated at 1400° C was completely changed as shown in Fig. 5. In the interior of the grains this microstructure is characteristic of eutectoid decomposition, whereas the white grain-boundary phase was m. TEM observation revealed that the c grains sometimes contain small t precipitates, interlaced with lamellar shaped MgO-rich phase. The latter phase was proved to be forsterite (Mg_2SiO_4) using diffraction patterns for analysis.

TEM observations were unable to confirm changes in the volume fraction of the conventional

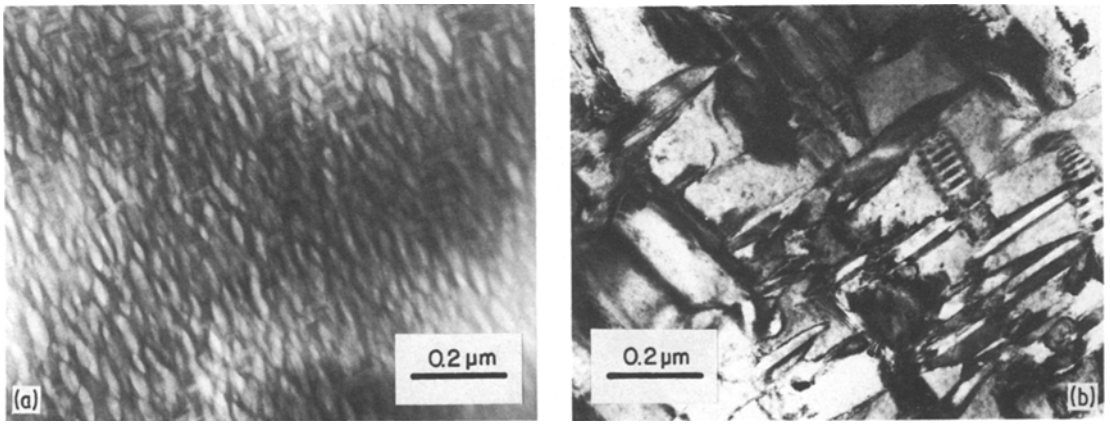

Figure 2 (a) Ellipsoidal shaped t precipitates distributed homogeneously and oriented crystallographically in the c matrix. (b) Lenticular shaped t precipitates of larger size often transform to the m symmetry by internal twinning.

*JEOL 100-CX.

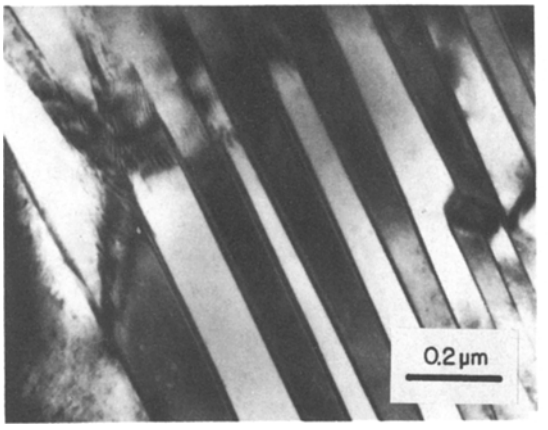

Figure 3 Large m twins formed during cooling after sintering.

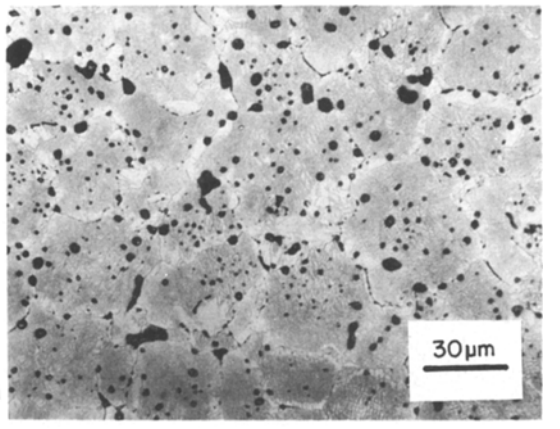

Figure 5 The eutectoid decomposition in c areas involving forsterite (Mg_2SiO_4) lamellae. The white grain-boundary m phase is also present. Annealed at 1400° C/120 h.

phases (c, t, m) in the specimens heat treated at lower temperatures, due to the wide range of inhomogeneity which exists in these specimens. However, tilting experiments showed appreciable strain-field contrast around small t precipitates, where these appeared in clusters or in a complete c grain (Fig. 6). The appropriate SAD patterns from these areas revealed the ordering phenomena, which is characterized by strong superlattice reflections. Such diffraction patterns from different zone-axes are presented in Fig. 7. The ordering process results in the formation of the β-phase ($Mg_2Zr_5O_{12}$). This phase is one of the fluorite-related homologous series R_nO_{2n-2} with $n = 7$ [7]. This was verified by observations through the $[1\,1\,2]_c$ zone-axis (Fig. 7a). This zone-axis coincides with the simplest zone-axis of the β-phase, namely $[0\,0\,1]_R$ (rhombohedral notation).

The rhombohedral crystal structure of $a_R = 0.618$ nm, $\alpha_R = 99.58°$ and a symmetry group of $R\bar{3}$ reported for this phase [8], as a high temperature phase. This structure is derived from the fluorite structure by ordering of the oxygen anion vacancies along a specific ⟨1 1 1⟩ direction of c fluorite phase. The lattice volume is 7/4 times the fluorite parent. The cations are in a completely disordered state in the rhombohedral cell of $Mg_2Zr_5O_{12}$ [9], thus this phase has a metastable character and its formation is a result of closely matching cationic radii, high anionic mobility and the stability of the oxygen vacancy pairs. These characteristics are in turn related to the nature of the formation of this phase.

An appropriate orientation relationship between the β-phase and the c matrix was derived from the diffraction patterns and is shown in Fig. 8. By

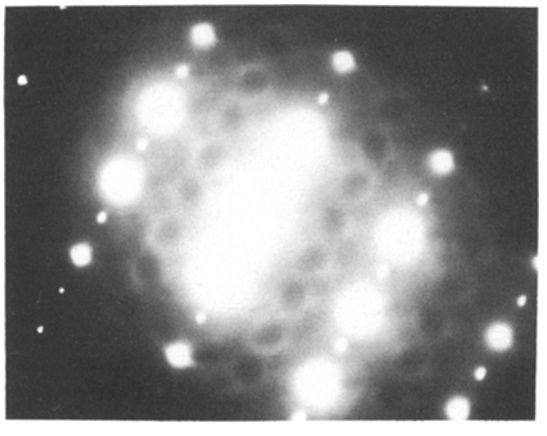

Figure 4 Diffuse scattering intensity (DSI) which is characteristic of c grains containing t precipitates. Zone axis = $[0\,1\,3]_c$.

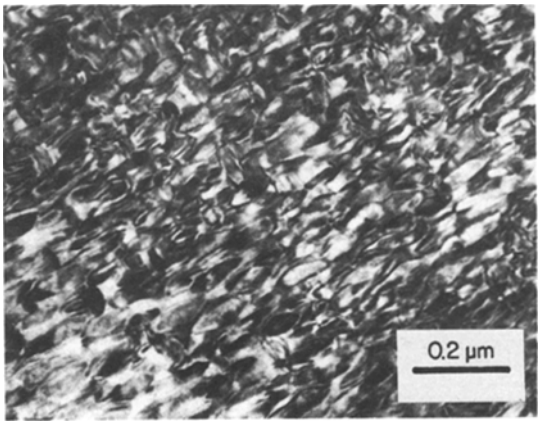

Figure 6 Strain-field contrast around t precipitates in a specimen heat treated at 900° C/20 h.

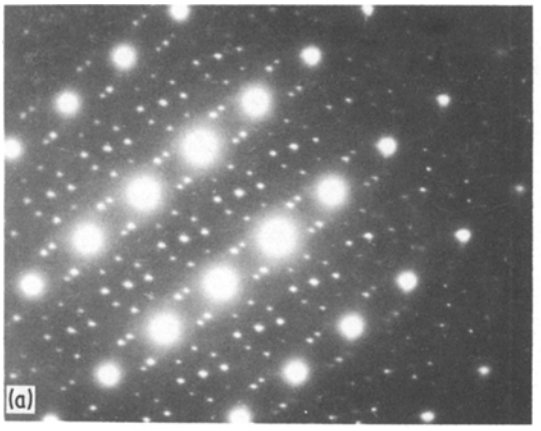

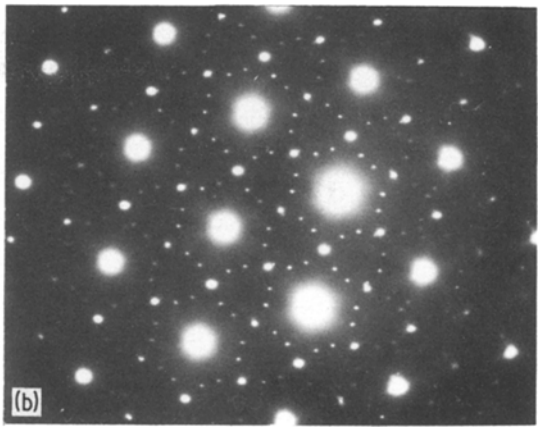

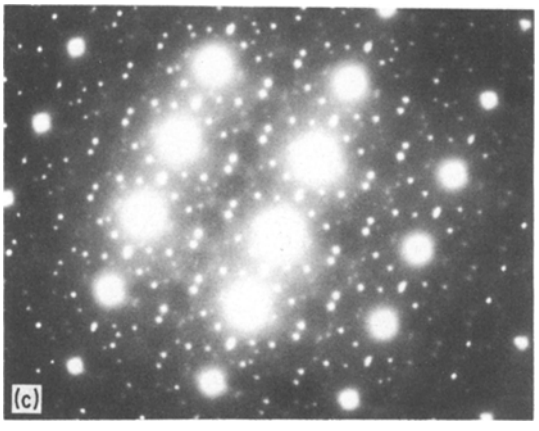

Figure 7 Selected-area diffraction patterns (SADP) from the ordered regions between t precipitates. (a) Zone axis = $[1\,1\,2]_c$. (b) Zone axis = $[1\,1\,1]_c$. (c) Zone axis = $[0\,1\,3]_c$.

observation of a number of diffraction patterns the twin-related reflections of the β-phase were observed, with $(2\,2\,0)_c$ as the habit plane. The separation of the twin system is shown schematically in Fig. 9 for a $\langle 1\,1\,2\rangle_c$ zone-axis.

In addition, many low intensity reflections appeared. These were related to the crystallographically different variants of the β-phase within the c matrix (overall, eight variants). The scattering amplitudes of these variants could be different and possibly low for a given zone-axis. Fig. 10 shows two dark-field micrographs from the same area as Fig. 6, using different variant reflections of the β-phase. Superposition of these two images still leaves many dark regions between the t precipitates, suggesting the existence of other β-phase variants in the same grain.

In regions where the ordered β-phase has been observed, the DSI phenomenon was absent in the diffraction patterns of the c matrix. In addition, several regions of discontinuous precipitation (cellular precipitation) of MgO-rich pipes, as reported by Hannink [5], were observed (Fig. 11). These were believed to be due to MgO-rich regions which exist as inhomogeneities in the material.

The eutectoid decomposition of 1400° C was composed of c, t and forsterite (Mg_2SiO_4) as verified from diffraction patterns. The forsterite is most probably a product of SiO_2 impurities reacted at high temperature with MgO-rich regions. No ordering process was found after heat treatment at 1400° C.

4. Discussion

The results for the temperature range 900 to 1100° C indicate that the microstructural changes are on the short-range scale in these specimens.

The absence of DSI in diffraction patterns taken from the ordered regions is in good agreement with the expected ordering process. As reported previously [10], the DSI is distributed on oval surfaces, located along the $\langle 1\,1\,1\rangle$ directions in the c reciprocal lattice. These surfaces were related to vacancy pairs which caused trigonal (rhombohedral) symmetry relaxation of the fluorite structure. Different sections of these DSI surfaces could be imaged in detail by observation through the various orders of the Laue zones in an electron diffraction pattern.

During the ordering process, the DSI surfaces convert to locally intense spots at discrete locations on these surfaces. These spots belong to the different variants of the ordered phase which contribute in the reciprocal lattice and for a given zone-axis the different variants generate intense reflections instead of diffuse intensity. Therefore,

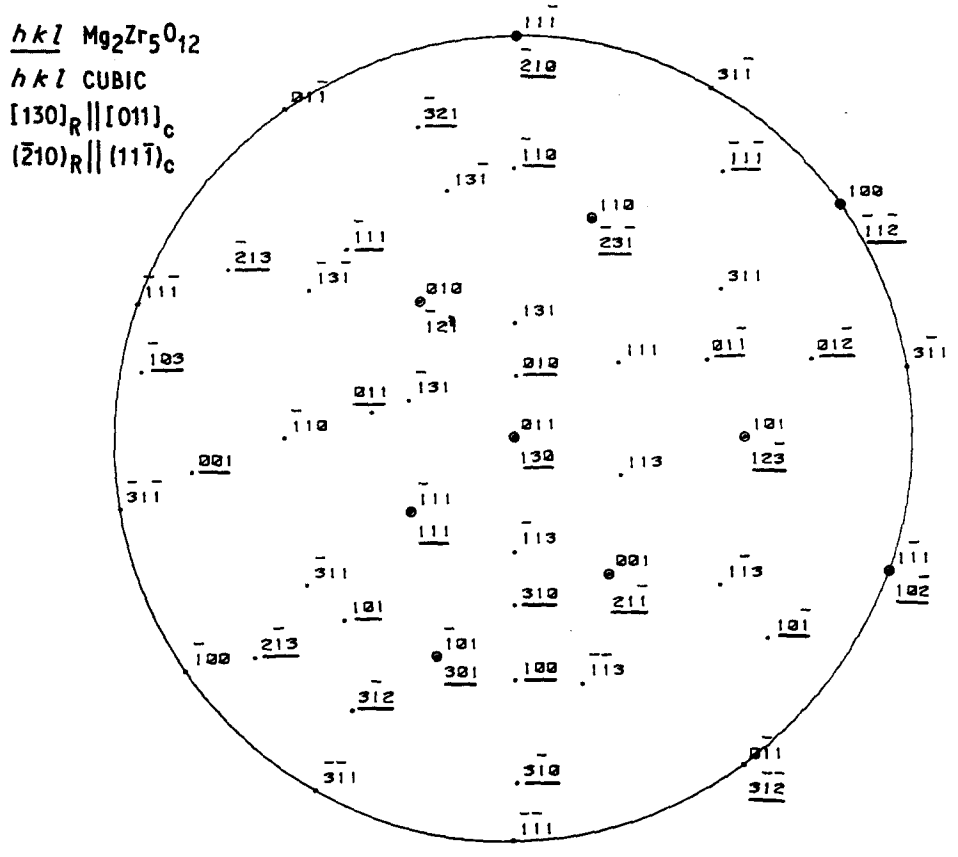

Figure 8 Combined stereographic projections for the c and β-phase (rhombohedral), indicating the orientation relationship between the two phases.

intense reflections of different β-phase variants could also be observed on different sections through c reciprocal lattice. By observation of different sections through reciprocal lattice, the DSI shapes could be made to coincide with the line profile formed by different β-phase variant reflections. This is in good accord with the transformation of the c grains from the disordered state as characterized above, to the ordered state, presumably caused by short-range diffusion.

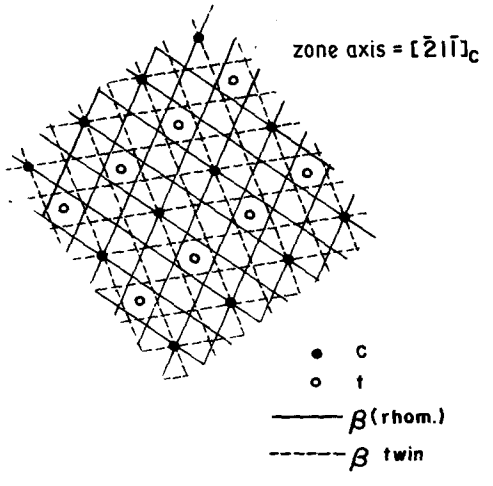

Figure 9 Schematic separation of the β-phase and its twin relative to the c and t reflections.

The formation of this metastable β-phase is postulated as follows: Fig. 12a represents the tentative concentration profile of the stabilizing cation across a t precipitate, a t–c interface and the c matrix, for an isothermal heat-treatment. In the c solid-solution phase-field of the ZrO_2–MgO phase diagram (Fig. 13), the c matrix has an average concentration, C_0. In the first stage of t nucleation in the t+c two-phase region, the local concentration should be c_t. The growth of the t precipitates, which is diffusion-controlled [11], is achieved by depletion of the stabilizer cation into the c matrix. This enrichment of the c matrix makes the presence of a concentration barrier a necessary condition for the diffusion process (there should be a positive concentration gradient). This barrier is shown by the solid curve in Fig. 12a. Further growth of the t precipitate

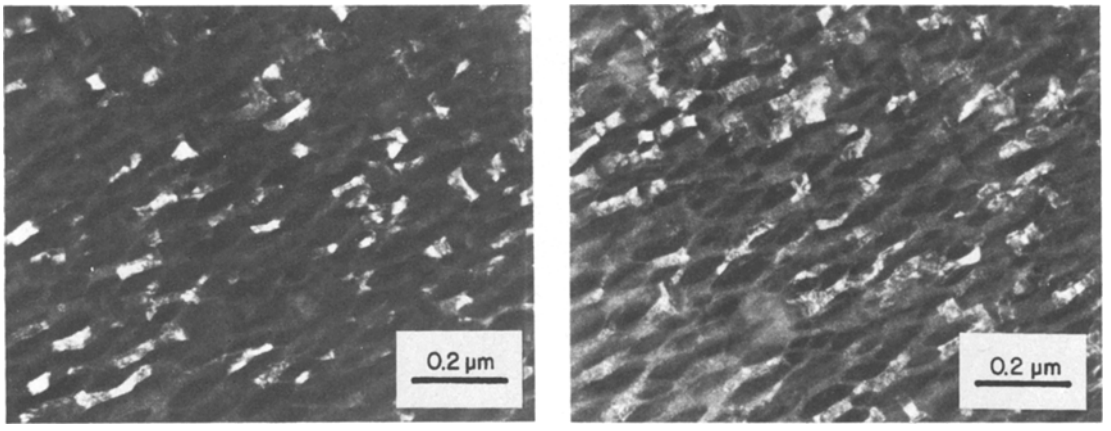

Figure 10 Dark-field micrographs of same area shown in Fig. 6, using different variant reflections of the β-phase.

requires the movement of the t–c interface, and is accompanied by a decrease of this concentration barrier as demonstrated by the dashed curve. The final equilibrium state would be achieved with the compositions of c_t and c_c for the t and c phase, respectively, as shown by the dotted curve.

For a given average bulk concentration (i.e. 9 mol % MgO), the concentration barrier decreases with increasing diffusion time and temperature. The increase in diffusion time is associated with the short-range homogenization of the c matrix ahead of the t–c interface, and a flattening of the "concentration hill". An increase in the diffusion temperature is associated with higher diffusion rates for the stabilizer cation, and a lower effective concentration barrier to the diffusion process. Increasing the diffusion temperature thus results the flattening of the "concentration hill".

There is a high local stabilizer concentration in the c matrix, near the t–c interface, which is a non-equilibrium state for the bulk of the specimen. However, this step could be considered as the "pseudo-equilibrium state" in specific conditions. These conditions may be described for the PSZ used for this work. The commercial 9 mol % MgO–PSZ is located on the dashed vertical line in the ZrO_2–MgO phase diagram [12] shown in Fig. 13.

Sintering in the two-phase region (c + t) has generated the c matrix containing the t precipi-

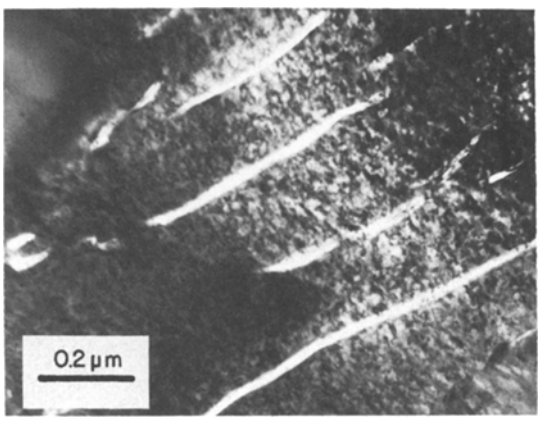

Figure 11 MgO-rich pipes as a product of discontinuous decomposition associated with MgO-rich c regions.

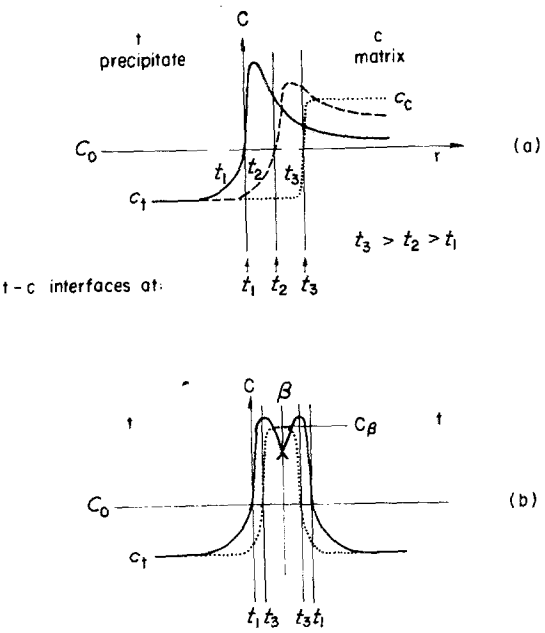

Figure 12 (a) Schematic stabilizer concentration profile across the t–c interface as a function of heat-treatment time. (b) Overlapping of the "concentration hills" of adjacent t precipitates to form a matrix with saturated c_β concentration.

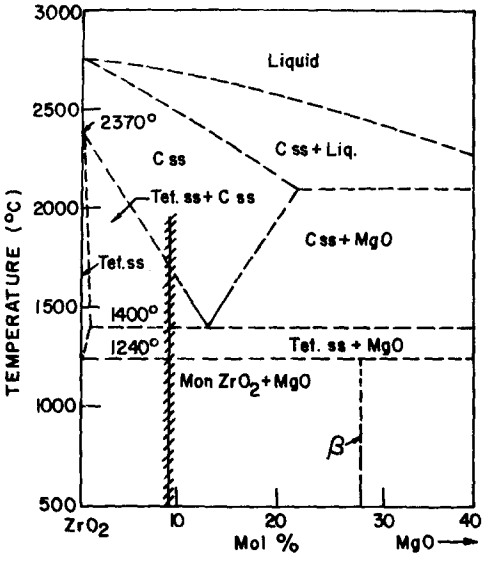

Figure 13 The ZrO_2–MgO phase diagram [12]. The commercial PSZ is indicated by dashed lines. The hypothetical location of the β-phase is also given.

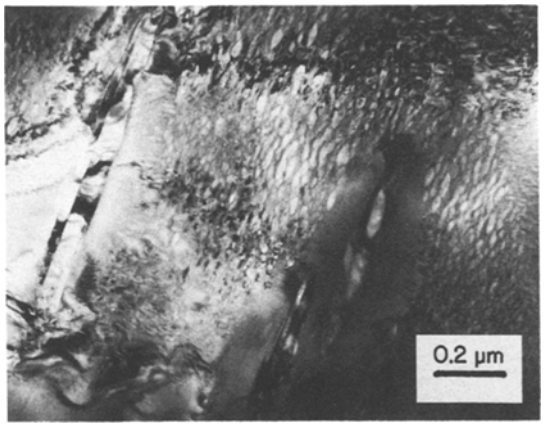

Figure 14 The dissociation process of locally equilibrated clusters leading to complete equilibrium with the surrounding microstructure.

tates, and large m twins formed during cooling. This was confirmed by the TEM observations in Section 3. The post-sintering heat treatment does not include a solution heat treatment and was thus distinct from the ageing process. Hence the wide range of the t precipitate size. In addition, where the t precipitates were very small, a high density has been observed in the c grains. If the interparticle distance of these t precipitates is small enough, it is possible for "concentration hills" of adjacent t precipitates to overlap as shown schematically in Fig. 12b by the solid curves. This leads to the locally final saturation concentration c_t, and $C_\beta (C_\beta > C_c)$ as shown by the dotted line. Further growth of the t precipitates is then retarded, a state which should be equivalent to local "pseudo-equilibrium".

At high temperatures (above 1200° C) diffusion of the stabilizer cation (Mg^{2+}) is rapid enough to ensure dissolution of such regions by long-range homogenization, to achieve the equilibrium state throughout the bulk of the specimen. Such a homogenization process is shown in Fig. 14. The characteristic feature is shown by the existence of clusters in the c grains, containing small t precipitates. The surrounding area of the clusters is c containing isolated and bigger t particles. The clusters are locally in the pseudo-equilibrium state, while the equilibrium state for the bulk would be achieved by peripheral dissolution of these clusters. This could also occur at lower temperatures for relatively long heat-treatment periods, as confirmed by Hannink's data [5] for 1100° C.

At temperatures below 1200° C, the diffusion rate of the stabilizer cation is low. Therefore, cluster dissolution can not occur due to the limited diffusion distance. However, the stabilizer cation could still diffuse for short distances. This, together with the tendency towards oxygen vacancy ordering in fluorite-type structures, could lead to the formation of an ordered fluorite-related compound, providing an appropriate concentration level of C_β is achieved.

If this compound determines the boundary of the two-phase region (m + compound) as assigned hypothetically on Fig. 13, then the formation and stabilization of this phase would be favoured.

Although there are no data for the diffusion coefficients of Mg^{2+} in ZrO_2, phase-stability experiments [12, 13] support the above assumptions about the diffusion behaviour in different temperature ranges.

From this tentative model, one can understand the observed ordering process. The formation of the β-phase occurs by a stabilizer concentration redistribution which causes the formation of ordered regions initiating from the t–c interface and propagating into the c matrix. The stabilizer concentration level is the controlling parameter, although full ordering in the β lattice may not be achieved. Thus, there is no actual interface for this solid state reaction. This explains the subsequent heterogeneous nucleation of β at t–c interfaces as suggested by Heuer *et al.* [15] and Hannink [5],

TABLE I Physical parameters of c, t and β-phase in 9 mol % MgO–PSZ

	Cubic	Tetragonal	β-$Mg_2Zr_5O_{12}$
Lattice parameter (nm)	$a = 0.5085$	$a = 0.5072$ $c = 0.5183$	$a = 0.618$ $\alpha = 99.58°$
Lattice volume (nm^3)	0.131 48	0.133 33	0.128 49*
Relative lattice volume change (%)	$\frac{V_c - V_t}{V_c} = -1.4$		
	$\frac{V_\beta - V_t}{V_\beta} = -3.7$		
Misfit parameter $\delta = \frac{d_i - d_j}{d_i}$	$\frac{d_c - d_t}{d_c} = -4.4 \times 10^{-3}$		
for (1 1 1) d-spacing	$\frac{d_\beta - d_t}{d_\beta} = -12.0 \times 10^{-3}$		

*Normalized to fluorite lattice by multiplying factor: 4/7.

although we believe that the concentration profile is responsible for this rather than the surface free-energy term, as in conventional heterogeneous nucleation.

Farmer *et al.* [16] have used two-step heat-treatments at lower (800° C) and high temperatures (1100° C) in order to form the β-phase. However, the fact that the β-phase formed at 900° C for longer times (20 h) in our experiments and in those of Hannink [5] at 1100° C for 2 h, indicates that the two-step process is not essential. Furthermore, the interparticle distances in the ordered regions in our experiments and in other work [5, 14, 16] are in the range of < 30 nm, while no work has reported this ordering process on a coarser scale. This fact supports our explanation which suggests that the concentration profile is responsible for the β-phase formation.

The formation of β-phase is restricted to specific regions where small t precipitates exist and this together with the small scale of β-phase distribution, should account for the relatively small volume fraction of this phase. This is probably the principal reason why the β-phase could not be detected by X-ray experiments.

The information of the β-$Mg_2Zr_5O_{12}$ phase has important effects on the stabilization of the t precipitates. First, the retardation of the t growth as mentioned earlier is due to the limited diffusion of the stabilizer cation. Therefore, the size of the t precipitates is limited, a fact which favours t stability with respect to the t → m transformation. (The size parameter is involved in the balance between the surface free energy and volume free energy terms in the total free energy change for the t → m transformation.)

Secondly, the change of the molar surface free energy (γ) of the t precipitates is also affected, due to the change of the adjacent c matrix to β-phase. Although the sign of this change is not known, this effect undoubtedly exists. The derivative effect from the interfacial energy change is the misfit at the t–β interface, which is associated with the lattice parameter of the β-phase.

The orientation relationship of the c matrix and β-phase (see Fig. 8) together with that of c matrix and the t precipitates [6], together result in the coherent boundary of the t precipitates and the β-phase. This was supported by the strain field contrast observed around the t particles.

For the c, t and β (rhombohedral), the (1 1 1), interplanar spacing has been considered the best comparative indication for the lattice misfits of these structures. The calculated misfit parameters for the two cases were compared in Table I. The results indicate an increase in the coherency misfit by a factor of 2.7 for the t–β interface relative to that of the t–c interface. This increase was observed qualitatively from the change of strain-field contrast around the t precipitates for a given zone-axis. This misfit enhances the destabilization of the t particles in the t → m transformation, by eliminating the particle size for which coherency is retained.

The relative lattice volume change was also decreased by the same factor (see Table I) indicating the reliability of the (1 1 1) *d*-spacing for representing the average misfit parameters of different phase pairs. The decrease in the lattice volume of β-phase relative to that of c phase is in accordance with the relaxation of the fluorite structure by the formation of oxygen vacancy strings. However, this could affect the matrix constraint response to the volume change which would be induced by the t → m transformation, and could result in a decrease in the toughening effect.

However, this phase has only been formed in "pseudo-equilibrium", presumably for broad composition range. It is, therefore, necessary to determine the compositions and temperature ranges in which the β-phase is stable.

Acknowledgement

This work was in part performed at MPI für Metallforschung, Stuttgart, West Germany.

References

1. G. K. BANSAL and A. H. HEUER, *J. Amer. Ceram. Soc.* **58** (1975) 235.
2. D. L. PORTER and A. H. HEUER, *ibid* **62** (1979) 298.
3. L. H. SCHOENLIEN, PhD thesis, Case Western Reserve University, Cleveland, Ohio, USA (1981).
4. R. H. J. HANNINK and R. C. GARRIE, *J. Mater, Sci.* **17** (1982) 2637.
5. R. H. J. HANNINK, *ibid.* **18** (1983) 547.
6. *Idem, ibid.* **13** (1978) 2487.
7. P. KUNZMANN and L. EYRING, *J. Solid State Chem.* **14** (1975) 229.
8. O. YANOVITCH and C. DELAMARRE, *Mater. Res. Bull.* **11** (1976) 1005.
9. H. J. ROSSELL and H. G. SCOTT, *J. de Phys.* **C7** (12) (1977) 28.
10. R. CHAIM and D. G. BRANDON, Proceedings of the Second International Conference on the Science and Technology of Zirconia, June 1983, Stuttgart, West Germany (1983).
11. D. VIECHNICKI and V. S. STUBICAN, *J. Amer, Ceram. Soc.* **48** (1965) 292.
12. C. F. GRAIN, *ibid.* **50** (1967) 288.
13. P. DUWEZ, F. ODELL and F. H. BROWN Jr, *ibid.* **35** (1952) 107.
14. R. H. J. HANNINK and M. V. SWAIN, *J. Aust. Ceram. Soc.* **18** (2) (1982) 53.
15. A. H. HEUER, H. H. SCHOENLEIN and S. C. FARMER, Proceedings, Conference on Science of Ceramics 12, June 1983, Saint Vincent, Italy (1983).
16. S. C. FARMER, L. H. SCHOENLEIN and A. H. HEUER, *J. Amer. Ceram. Soc.* **66** (7) (1983) C-107.

Received 27 October
and accepted 24 November 1983